Hindawi
Advances in Materials Science and Engineering
Volume 2021, Article ID 5534917, 13 pages
https://doi.org/10.1155/2021/5534917

Research Article

Experimental Study on the Effect of Boric Acid Corrosion on the Performance of Reinforced Concrete

Qianying Wang,[1] Jigang Zhang,[2,3] Mingchao Shan,[4] Bingying Yu,[4] Yang Zhao,[5] and Ran Yang[2]

[1]*College of Civil Engineering & Architecture, Qingdao Agricultural University, Qingdao, Shandong, China*
[2]*College of Civil Engineering, Qingdao University of Technology, Qingdao, Shandong, China*
[3]*Cooperative Innovation Center of Engineering Construction and Safety in Shandong Blue Economic Zone, Qingdao, China*
[4]*Shandong Nuclear Power Co. Ltd., Haiyang, Shandong, China*
[5]*Qingdao Gong High-Tech Material Co. Ltd., Qingdao, Shandong, China*

Correspondence should be addressed to Jigang Zhang; jigangzhang@126.com

Received 25 February 2021; Accepted 4 June 2021; Published 19 June 2021

Academic Editor: Shengwen Tang

In this study, the effect of boric acid in the cooling water system of nuclear power plants on the durability of reinforced concrete was experimentally studied. The mechanical properties of reinforced concrete under boric acid solution environments were studied by accelerated test methods. In addition, the effect of boric acid on the electrochemical behavior of steel bar and microstructure of concrete was studied. The results showed that boric acid corrosion does not affect reinforced concrete to a large extent, as corrosion only occurs on the surface of reinforced concrete, and thus, the internal reinforced concrete still maintains a high alkaline environment. At a boric acid concentration of 3%, corrosion products are crystallized on the surface of the specimen, which inhibits further corrosion.

1. Introduction

Boric acid, as a nuclear reactor moderator, is widely used in the cooling water system of nuclear power plants. With the increasing service time of nuclear power plants, the leakage of boric acid solution from the cooling water systems has gradually become an apparent problem. Besides, the impact of boric acid corrosion on the safety of nuclear power plant structures has become an issue of great concern.

Nuclear power plant structures have high importance and should have a long service life. In general, they are constructed of reinforced concrete. In recent years, some nuclear power plant structures have also been constructed using steel plate concrete structures [1]. Boric acid plays an important role in the cooling water system for nuclear fuel reactivity control and is present in the primary loop cooling water, which is in direct contact with the core and nuclear fuel. In addition, it is also present in the in-containment refueling water storage tank (IRWST) and spent fuel pool, which are constructed with reinforced concrete with stainless steel coating. The operating characteristics of the nuclear power plant do not allow IRWST and spent fuel pool to be emptied frequently for inspection, and thus, liquid leakage from them will have the long-term effect of boric acid corrosion on concrete. Therefore, the effect of boric acid corrosion on reinforced concrete needs to be studied in a systematic way.

In recent years, many studies have been carried out on the durability of concrete materials and structures [2–6]. There have been no cases of overall structure destruction of the IRWST due to boric acid corrosion [7]; therefore, the effects of reinforced concrete properties in boric acid corrosion environments have been less investigated [8, 9]. Based on the main functional characteristics of the wet surface area of IRWST, Wu et al. indicated that the facing steel plate should have good mechanical properties, corrosion

resistance, and processing and welding properties [10]. Huang et al. conducted an experimental study on the basic mechanical properties of concrete under different concentrations of boric acid immersion environment, and the results showed a relatively weak effect of boric acid on mechanical properties such as compressive strength and elastic modulus of concrete [11]. Rong et al. drilled core samples on the site for nuclear power plants where boric acid solution leakage occurred and found that the corrosion of concrete by boric acid only occurred on the surface of the specimen. The corrosion products inside the concrete were not monitored, and the compressive strength of concrete in the corroded area was slightly reduced [12].

In this study, the effect of boric acid leakage on the performance of reinforced concrete was investigated in the actual environment of nuclear power station primary loop water, and the properties of reinforced concrete under the corrosion of boric acid were studied by laboratory simulation methods to investigate the corrosion effects of boric acid solutions on reinforced concrete.

2. Test Materials and Concrete Mixture Ratio

2.1. Test Materials. Portland cement (P.O42.5) was used as the cementitious material in this test. Natural fine aggregate was river sand with a fineness modulus of 2.98. The coarse aggregate was crushed stone with continuous gradation with particle sizes ranging from 4.75 to 19 mm and 19 to 37.5 mm. Class I fly ash, high-efficiency water reducing agent, and air-entraining agent were used in the test. Normal tap water was used for concrete mixing.

The test was conducted using ordinary hot-rolled ribbed seismic steel bars with diameters of 10, 16, and 20 mm for flexural test, mechanical properties of steel bars, and reinforced concrete bond strength test, respectively. A35 standard tensile specimens with a thickness of 5 mm were used for determining the basic mechanical properties of steel plates. The testing steel bar and steel plates used are shown in Figure 1.

2.2. Concrete Mix. The durability of concrete materials and structures is influenced by many factors, including the environment, aggregates, and additives [13, 14]. The concrete proportions used for the tests were in accordance with the Code Requirements for Nuclear Safety-Related Concrete Structure (ACI 349-01), with a water-cement ratio (W/C) of 0.59, a sand ratio of 41%, and a design slump of 150 ± 25 mm. The proportions used for the tests are the same as those used for nuclear island concrete in a nuclear power plant, with the aim of facilitating the use of the test results to guide operation and maintenance. The composition of the concrete mix is listed in Table 1.

3. Test Method

3.1. Test Environments. The mode of action and concentration of corrosion solution determine the degree of corrosion of reinforced concrete. For the purpose of the comparative study of the boric acid corrosion effect, a blank control group (distilled water environment) was set up. Considering the actual environment in the primary loop of the nuclear power plant, the concentration of the boric acid solution was chosen to be 0.27%. At the same time, in order to accelerate the corrosion rate of reinforced concrete, the test was also carried out with boric acid concentrations of 0.8% and 3%. In order to simulate the real environmental conditions, two test environments including immersion and alternating wet and dry conditions were established. The alternating wet and dry process cycle using corrosion solution involved soaking for four days and natural drying for three days. The IRWST operates at a temperature of approximately 55°C; therefore, the test was carried out at room temperature.

Figure 1: Testing rebar and steel plates.

3.2. Mechanical Property Test. The mechanical properties of steel plates and reinforced concrete including compressive strength, splitting tensile strength, and static elastic modulus of concrete, flexural strength, and bond strength were investigated. A total of 8 different test environments including 2 test conditions of immersion and alternating wet and dry and 4 different boric acid concentrations were set for each test condition. The reinforced concrete specimens were maintained under the standard conditions for 28 days and then placed in the corrosion solution with the descaled steel and steel plate specimens, and these tests were conducted every 2 months at 60 days, 120 days, 180 days, 240 days, and 300 days.

The compressive strength, splitting tensile strength, static elastic modulus, and flexural strength tests were conducted according to the standard test method for mechanical properties of ordinary concrete (GB/T 50081-2002). Cube specimens of $100\,\text{mm} \times 100\,\text{mm} \times 100\,\text{mm}$ were used to test the compressive and splitting tensile strengths. The static elastic modulus was determined using $100\,\text{mm} \times 100\,\text{mm} \times 300\,\text{mm}$ size specimens. Two ordinary hot-rolled ribbed seismic steel bars of 10 mm diameter were placed inside the reinforced concrete flexural test specimen with the specimen size of $100\,\text{mm} \times 100\,\text{mm} \times 400\,\text{mm}$. Transverse cracks of 0.2 mm were preset in the middle of the specimen by steel pieces.

The basic mechanical properties of the steel bars and steel plates were tested according to the tensile test of metal materials (GB/T 228.1-2010). The ordinary hot-rolled ribbed seismic steel bars with a diameter of 16 mm and A35 carbon steel plate with a thickness of 5 mm were used in this study [15].

Table 1: Concrete mixture ratio (kg/m^3).

Medium sand (0–4.75 mm)	Small-medium stone (4.75–19 mm)	Big stone (19–37.5 mm)	Cement	Fly ash	Water reducer (0.8%)	Air-entraining agent (0.003%)	Mixing water
734	581	475	273	91	2.912	0.0109	160

The reinforced concrete bond strength test was carried out according to the test specification for hydraulic concrete (SL 352-2006). A cube specimen of 150 mm × 150 mm × 150 mm was used, and an ordinary hot-rolled ribbed seismic steel bar of 20 mm diameter was placed at the center.

3.3. Microstructural Analysis of Concrete and Reinforcement. The corrosion products and microstructure of concrete were analyzed by the concrete powder at 0 and 2 cm below the concrete surface by X-ray scanning using a D8 ADVANCE series X-ray diffractometer (Bruker). The crushed concrete specimens were analyzed by scanning electron microscopy using a HITACHI S-3500N series scanning electron microscope.

The corrosion of reinforcing steel was analyzed through electrochemical impedance spectroscopy tests on the reinforcing bars in the flexural specimens using a PARSTAT 4000A series electrochemical workstation. The bars were derusted before pouring to avoid the original oxide film affecting the generation of passivation film of steel bars [16].

4. Test Results and Analysis

4.1. Effect on Mechanical Property of Concrete. The compressive strength, splitting strength, and elastic modulus of concrete under each environment are shown in Table 2. A group of three specimens was set up for each test environment and each age, and the average values of the mechanical properties of each group are listed in Table 2. The compressive strength, splitting strength, and elastic modulus loss rates were calculated based on the mechanical properties of distilled water (boric acid concentration 0%) immersion and dry-wet alternating groups, and the results are shown in Figure 2.

The maximum compressive strength loss rate of concrete was 5.04% at a boric acid concentration of 3% for 240 days in alternating wet and dry conditions. At a boric acid concentration of 3%, the compressive strength loss rate fluctuates at the late stage of corrosion, mainly because the corrosion products attached to the surface of the specimen are gradually uniform, and the stress concentration caused by the corrosion products gradually disappears.

The maximum loss rate of splitting tensile strength of concrete (3.94%) was observed at a boric acid concentration of 3% at 180 days of wet and dry alternation. No significant relationship was observed between the loss rate of splitting tensile strength and the concentration of boric acid at 60 days of corrosion in different concentrations.

The loss rate of concrete elastic modulus was less affected by the boric acid concentration. The maximum loss rate of concrete elastic modulus was 1.57% at a boric acid concentration of 3% at 240 days of alternating wet and dry conditions. The loss rate of elastic modulus in the alternating wet and dry environment at 0.27% boric acid concentration was the smallest and at 0.8% boric acid concentration was the same as that in the immersion environment at 0.27% boric acid concentration. The corrosion effect of boric acid on the concrete elastic modulus indicated a relatively weak corrosion effect of low concentration boric acid solution.

Figure 2 shows that the concrete compressive strength loss rate in the dry and wet alternating corrosion environment is greater than that in the immersion environment. The main reason is that the crystallization of boric acid during the drying process of the specimen increases the porosity of the concrete surface. At a boric acid concentration of 3% of 120 days, corrosion crystals began to appear on the surface of concrete specimens in both corrosive environments. The corrosion time of 120 and 180 days compared with the alternating wet and dry environment shows that the growth rate of compressive strength loss rate is relatively low under the immersion environment, mainly because more corrosion products adhere to the concrete surface in the immersion environment.

Figure 3 shows the surface of the test block after 300 days of corrosion in the presence of boric acid. At a corrosion age of 300 days, corrosion crystals appeared on the surface of concrete specimens under the immersion environment with a concentration of 0.8%, while the surface of specimens under alternating wet and dry environments remained bright and clean.

4.2. Effect on Mechanical Property of Reinforcement. The mechanical properties of steel bars and steel plates under each environment are shown in Tables 3 and 4. The yield and the ultimate strength loss rates of the steel bar and steel plate specimens with different corrosion times under immersion and alternating wet and dry environments only showed irregular fluctuations and no significant decrease in the test cycle, mainly because the corrosion rate of the steel bar and steel plate specimens is low, and the stress concentration caused by the cross-sectional dimensioning of the corrosion area does not occur during the test. The boric acid corrosive environment set up in the test has a low effect on the steel bar and steel plate. The yield and ultimate strengths of the steel bar and A36 steel plate specimens still meet the strength requirements during service.

The corrosion rate is the rate of mass loss of the specimens after corrosion. Tables 3 and 4 show that the overall corrosion rate of specimens is small and increases with time. The corrosion rate of the specimens in the alternating wet and dry environment was slightly higher than that in the soaking environment.

Table 2: Mechanical properties of concrete.

Test environment		Immersion			Dry-wet cycles		
Age (d)	Concentration (%)	Compressive strength (MPa)	Splitting tensile strength (MPa)	Elastic modules (10^4 MPa)	Compressive strength (MPa)	Splitting tensile strength (MPa)	Elastic modules (10^4 MPa)
60	0	60.0	3.90	3.54	58.3	3.78	3.52
	0.27	59.6	3.88	3.54	57.7	3.78	3.52
	0.8	59.3	3.89	3.54	57.2	3.76	3.51
	3	58.7	3.87	3.53	56.8	3.77	3.51
120	0	63.7	4.39	3.61	62.2	4.28	3.59
	0.27	63.0	4.36	3.60	61.1	4.24	3.58
	0.8	62.3	4.32	3.60	60.5	4.21	3.58
	3	61.5	4.29	3.59	59.7	4.17	3.56
180	0	66.9	4.66	3.67	64.7	4.57	3.65
	0.27	65.9	4.61	3.65	63.2	4.50	3.64
	0.8	64.9	4.58	3.65	62.5	4.46	3.64
	3	64.1	4.51	3.63	61.5	4.39	3.61
240	0	68.8	4.78	3.85	67.5	4.72	3.83
	0.27	67.7	4.72	3.82	66.0	4.65	3.81
	0.8	66.7	4.69	3.81	65.2	4.60	3.80
	3	66.0	4.63	3.80	64.1	4.55	3.77
300	0	69.6	4.85	3.92	69.0	4.83	3.91
	0.27	68.4	4.79	3.89	67.4	4.75	3.89
	0.8	67.5	4.76	3.88	66.7	4.71	3.88
	3	66.7	4.69	3.87	65.8	4.65	3.86

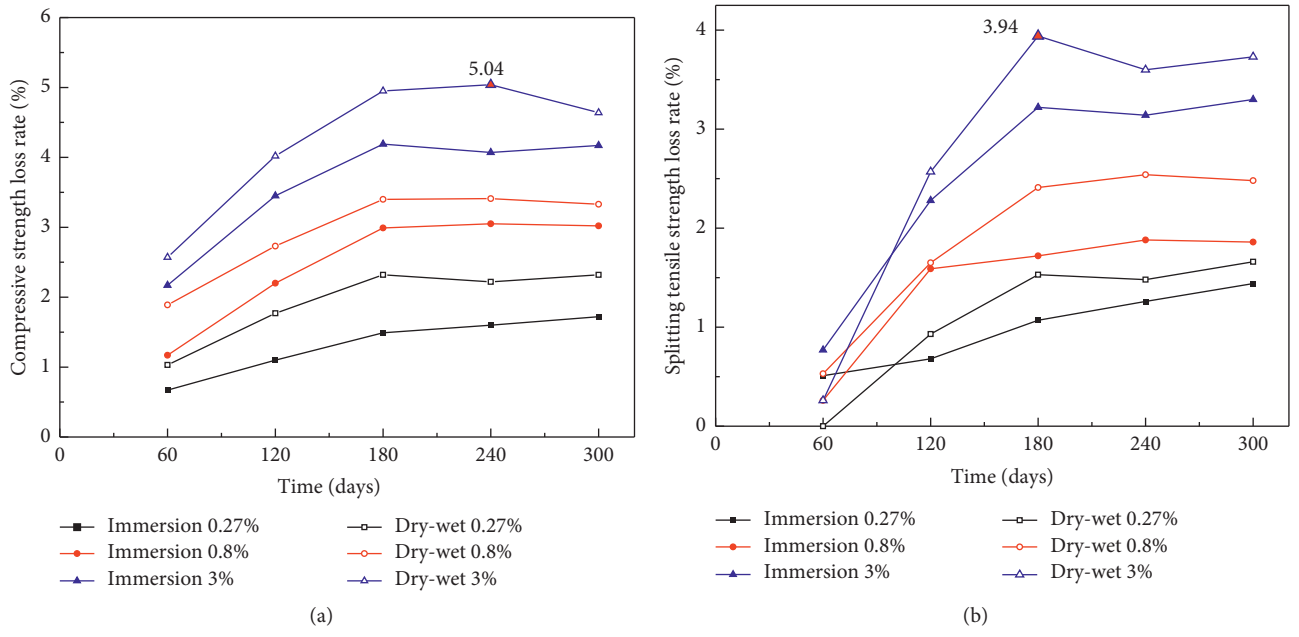

Figure 2: Continued.

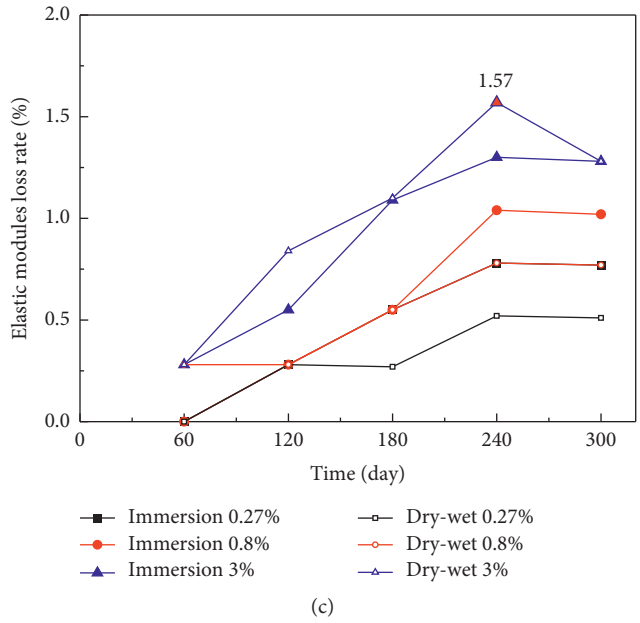

Figure 2: Loss rate of mechanical properties of concrete.

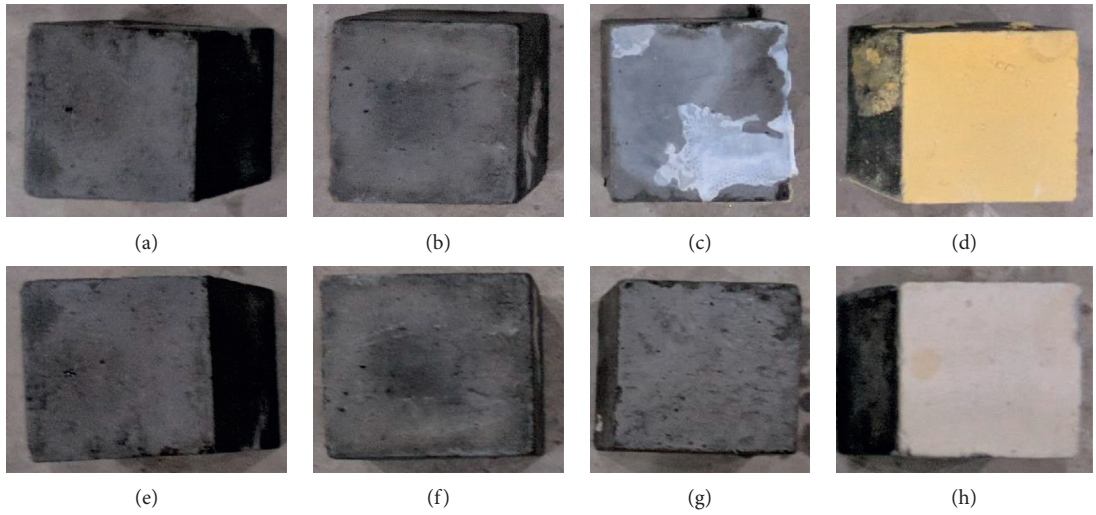

Figure 3: Concrete specimens after 300 days of corrosion: (a) immersion 0%, (b) immersion 0.27%, (c) immersion 0.8%, (d) immersion 3%, (e) dry-wet 0%, (f) dry-wet 0.27%, (g) dry-wet 0.8%, and (h) dry-wet 3%.

The steel bar and steel plate specimens at a corrosion test age of 300 days are shown in Figure 4. In the boric acid solution with a concentration of 3% after 120 days of corrosion, the surface of the steel specimen started being covered by corrosion products. When the corrosion age reached 300 days, after removing the corrosion products on the surface of the specimen, the internal steel bar and steel plates are only partially covered with black rust on the surface, while most areas remain bright. Combining the observed phenomenon with the mass loss of the steel bars and steel plates leads to the following observation:

(a) The effect of boric acid on steel is weak

(b) Corrosion products have a certain degree of denseness, inhibiting further corrosion of steel

4.3. Effect on Mechanical Property of Reinforcement Concrete. The flexural and bond strengths of reinforced concrete under each test environment are listed in Table 5. The mechanical properties of distilled water (boric acid concentration 0%) immersion and dry-wet alternating groups were used as the benchmark to calculate the loss rate of flexural strength and bond strength, and the results are shown in Figure 5.

The maximum flexural strength loss rate of the specimen was 3.57% at a boric acid concentration of 3% for 180 days in

Table 3: Mechanical properties of steel bar and steel plate in an immersion environment.

Test environment		Steel bar			Steel plate		
Age (d)	Concentration (%)	Yield strength (MPa)	Ultimate strength (MPa)	Corrosion rate (%)	Yield strength (MPa)	Ultimate strength (MPa)	Corrosion rate (%)
60	0	461.2	619.8	0.086	312.0	471.5	0.047
	0.27	460.7	619.6	0.086	312.3	471.2	0.063
	0.8	461.0	619.8	0.090	312.5	471.3	0.068
	3	461.2	620.0	0.092	312.5	471.2	0.078
120	0	461.2	619.8	0.113	312.5	471.5	0.063
	0.27	461.0	619.6	0.129	312.3	471.4	0.073
	0.8	461.0	619.6	0.132	312.2	471.4	0.078
	3	460.8	619.6	0.139	312.3	471.2	0.089
180	0	461.1	620.0	0.135	312.4	471.6	0.094
	0.27	461.0	619.7	0.140	312.6	471.3	0.100
	0.8	461.0	619.7	0.148	312.0	471.5	0.109
	3	461.0	619.7	0.146	312.4	471.2	0.099
240	0	462.0	620.3	0.160	312.3	471.4	0.120
	0.27	461.5	619.3	0.166	312.8	471.5	0.131
	0.8	460.8	620.0	0.174	312.1	471.1	0.146
	3	461.2	620.5	0.180	312.5	471.3	0.125
300	0	460.5	618.9	0.176	312.0	470.0	0.156
	0.27	460.0	618.5	0.170	312.2	470.5	0.172
	0.8	461.8	619.3	0.180	311.0	470.8	0.199
	3	459.7	619.6	0.158	311.6	471.0	0.121

Table 4: Mechanical properties of steel bar and steel plate under dry-wet cycles.

Test environment		Steel bar			Steel plate		
Age (d)	Concentration (%)	Yield strength (MPa)	Ultimate strength (MPa)	Corrosion rate (%)	Yield strength (MPa)	Ultimate strength (MPa)	Corrosion rate (%)
60	0	460.9	620.0	0.099	312.3	471.5	0.073
	0.27	461.0	619.7	0.101	312.0	471.0	0.079
	0.8	461.3	619.6	0.105	312.5	471.3	0.099
	3	461.0	620.1	0.107	312.5	471.3	0.120
120	0	461.2	619.8	0.137	312.1	471.2	0.121
	0.27	461.0	619.8	0.144	312.4	471.2	0.131
	0.8	460.9	619.8	0.148	312.0	471.0	0.142
	3	461.0	619.6	0.153	312.3	470.8	0.151
180	0	460.8	619.3	0.164	312.4	471.6	0.157
	0.27	461.2	619.5	0.171	312.4	471.7	0.162
	0.8	461.0	619.0	0.185	312.2	471.0	0.173
	3	460.8	619.6	0.167	312.3	471.4	0.167
240	0	461.3	619.0	0.190	312.5	471.7	0.183
	0.27	461.0	619.3	0.188	312.0	471.5	0.194
	0.8	461.5	618.8	0.191	311.8	471.2	0.197
	3	460.9	619.5	0.185	312.2	471.1	0.183
300	0	459.8	619.0	0.212	312.0	470.5	0.193
	0.27	460.7	618.7	0.236	311.8	470.6	0.236
	0.8	460.4	619.1	0.235	311.9	470.0	0.229
	3	459.3	619.4	0.201	311.5	470.4	0.193

alternating wet and dry conditions. The difference in the flexural strength loss rate of the specimens was small for the test environments with the boric acid concentration of 0.27% and 0.8%. The flexural strength loss rate is basically the same in the alternating environment of 0.27% concentration and the immersion environment of 0.8% concentration but showed large fluctuations in the later part of the test at a 3% boric acid concentration environment.

The loss rate of bond strength of specimens was small. The maximum loss rate of bond strength occurred at 240 days of corrosion under the wet and dry alternation, but the maximum value was only 1.83%, and the loss rate of bond strength tended

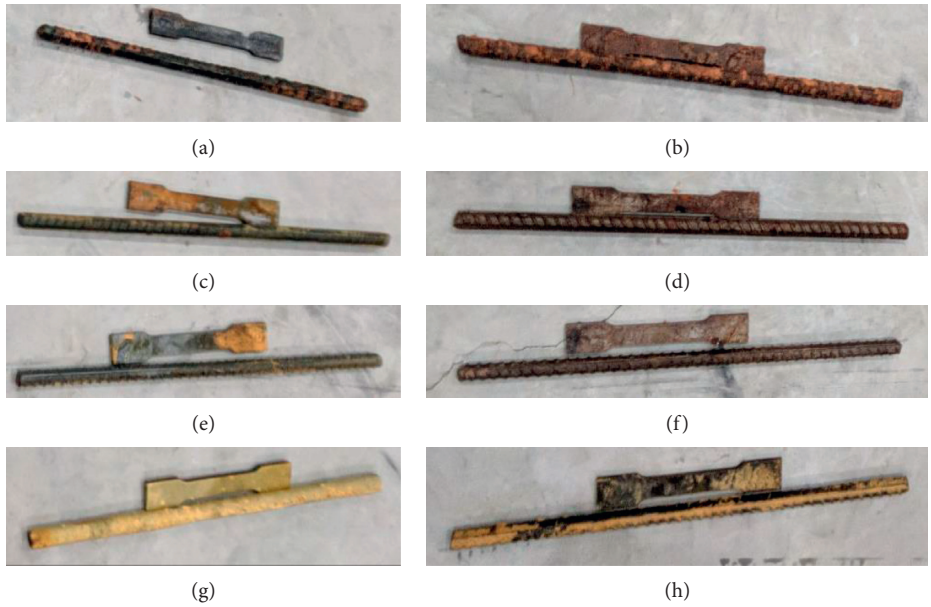

Figure 4: Steel bar and steel plate specimens after 300 d of corrosion: (a) immersion 0%, (b) dry-wet 0%, (c) immersion 0.27%, (d) dry-wet 0.27%, (e) immersion 0.8%, (f) dry-wet 0.8%, (g) immersion 3.0%, and (h) dry-wet 3.0%.

Table 5: Mechanical properties of reinforced concrete.

Test environment		Immersion		Dry-wet cycles	
Age (d)	Concentration (%)	Bond strength (MPa)	Flexural strength (kN)	Bond strength (MPa)	Flexural strength (kN)
60	0	7.62	21.6	7.56	20.8
	0.27	7.61	21.6	7.56	20.6
	0.8	7.61	21.4	7.54	20.7
	3	7.59	21.3	7.54	20.5
120	0	7.87	24.2	7.70	23.7
	0.27	7.85	24.0	7.67	23.4
	0.8	7.82	23.9	7.64	23.3
	3	7.79	23.6	7.60	23.0
180	0	8.05	25.4	7.96	25.2
	0.27	8.02	25.1	7.91	24.8
	0.8	7.96	24.0	7.88	24.6
	3	7.93	24.6	7.82	24.3
240	0	8.21	25.8	8.18	25.5
	0.27	8.17	24.5	8.12	25.0
	0.8	8.10	25.3	8.06	24.9
	3	8.08	25.0	8.03	24.6
300	0	8.27	25.6	8.28	25.7
	0.27	8.23	25.2	8.23	25.2
	0.8	8.20	25.1	8.19	25.1
	3	8.15	24.7	8.13	24.9

to be fixed at the later stage of corrosion. The bond strength of reinforced concrete was weakly affected by boric acid.

The test specimens of flexural strength and bond strength after 300 days of boric acid corrosion are shown in Figures 6 and 7. When the test specimens of flexural strength were split and sprayed with phenolphthalein solution, except for the surface location where no color indication appeared, the interior of the test specimens still maintained the high alkaline environment turning the phenolphthalein solution to red, and the internal reinforcement of the test specimens still maintained the polished luster. The internal reinforcement of the bond strength specimen also maintained the same pitting luster. The effect of boric acid corrosion on reinforced concrete specimens occurred only on the surface location of the specimen, and the internal reinforcement was not affected by the boric acid solution.

The electrochemical impedance spectra of the steel bars in flexural specimens of different ages under each corrosive

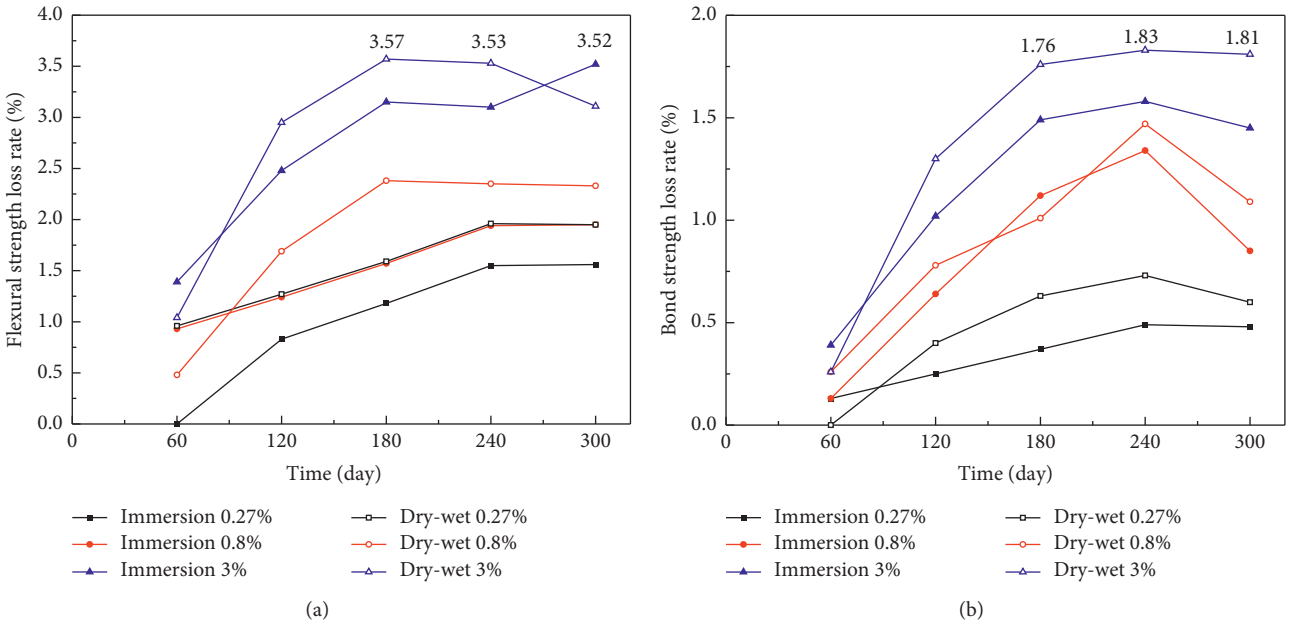

Figure 5: Loss rate of mechanical properties of reinforced concrete.

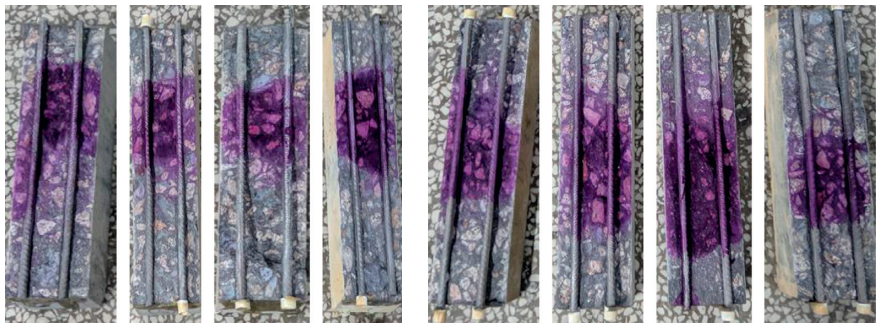

Figure 6: Flexural strength specimens after 300 days of corrosion: (a) immersion (0%, 0.27%, 0.8%, and 3%) and (b) dry-wet (0%, 0.27%, 0.8%, and 3%).

environment were recorded and analyzed. Figure 8 shows the Nyquist diagram of the internal reinforcement of the flexural specimen under the test environment, exhibiting only two capacitive resistance arcs in the high- and low-frequency regions.

The larger the radius of the low-frequency band capacitive arc, the greater the passivation film resistance of the steel surface [17, 18]. The intersection of the high- and low-frequency regions of the capacitive arc indicates the transfer resistance of the corrosive material to the surface of the reinforcement through the protective layer of concrete [19, 20].

The Nyquist diagram of the low-frequency band capacitive arc shows that under different corrosive environments, the slope of the low-frequency band capacitive arc resistance of the corrosion age of 60 days is significantly smaller than that after 120 days of corrosion. When the corrosion age reaches 120 days, there is no significant change in the slope of the low-frequency band capacitive arc resistance in different ages and corrosion environments. This result is consistent with the change in the cross-point position of the two capacitive resistance arcs in the real part of the Nyquist plot at different corrosion ages, probably because in the early stage of corrosion, relatively more cement is not fully hydrated inside the concrete, and the passivation film on the outer surface of the reinforcement is under a relatively weak alkaline environment. With increasing corrosion time, the internal cement hydrates more completely, providing a better alkaline environment for the internal reinforcement and the formation of a more complete passivation film on the surface of the reinforcement.

However, even in the early stages of corrosion, the low-frequency segment of the Nyquist plot in different corrosive environments does not show a flattened semicircular arc but a straight line with an inclination angle much greater than 45°. Similar test results were reported

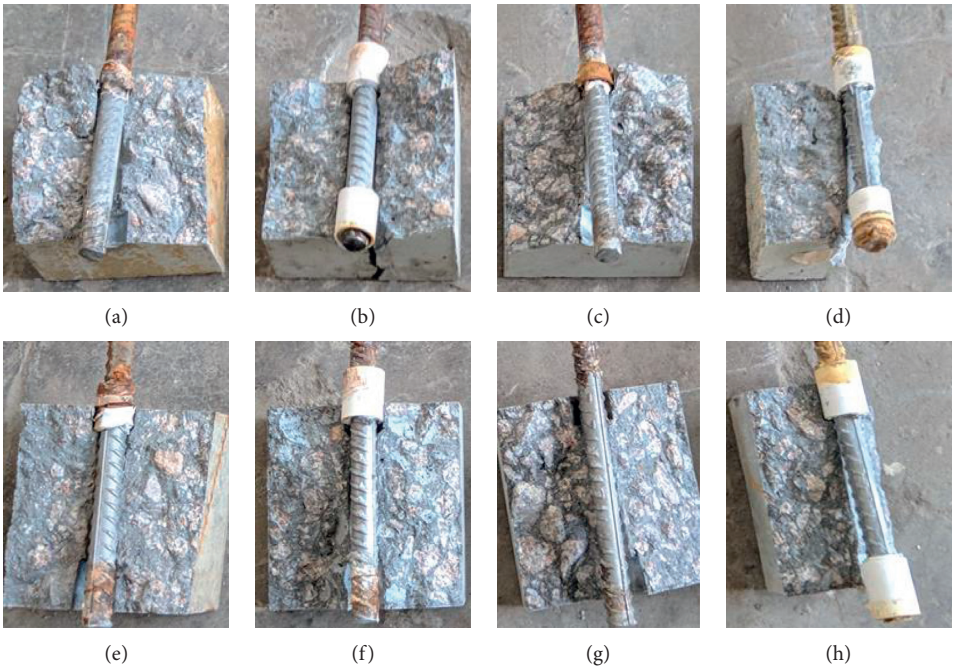

Figure 7: Bond strength specimens after 300 days of corrosion: (a) immersion 0%, (b) immersion 0.27%, (c) immersion 0.8%, (d) immersion 3%, (e) dry-wet 0%, (f) dry-wet 0.27%, (g) dry-wet 0.8%, and (h) dry-wet 3%.

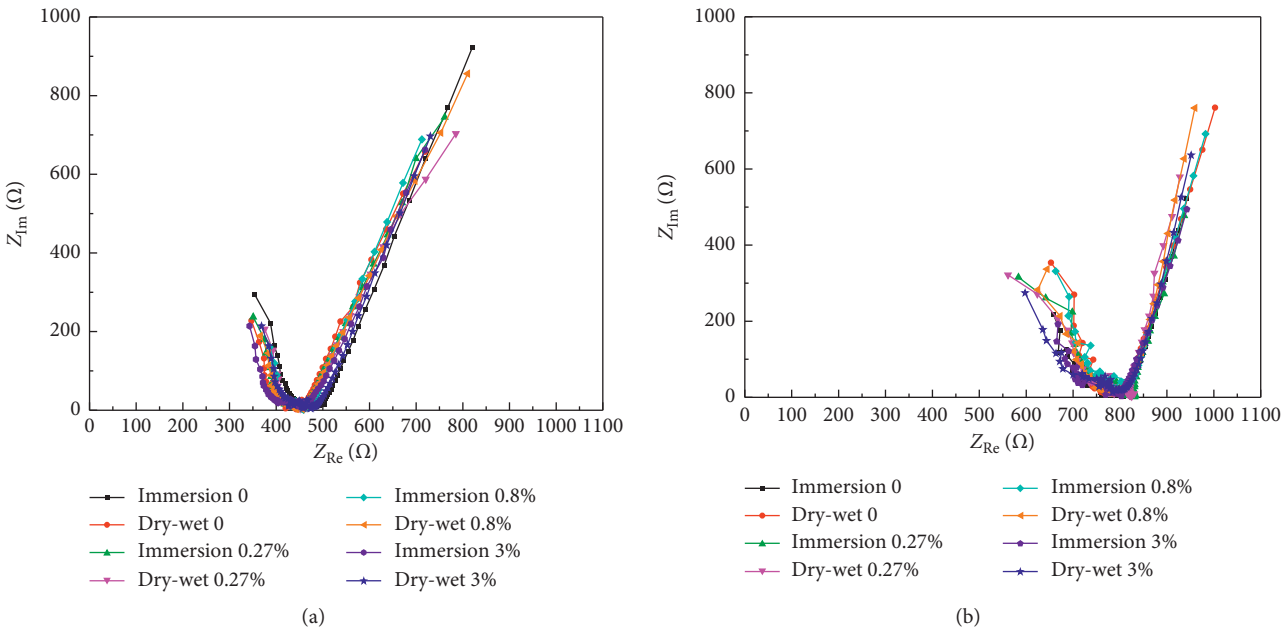

Figure 8: Continued.

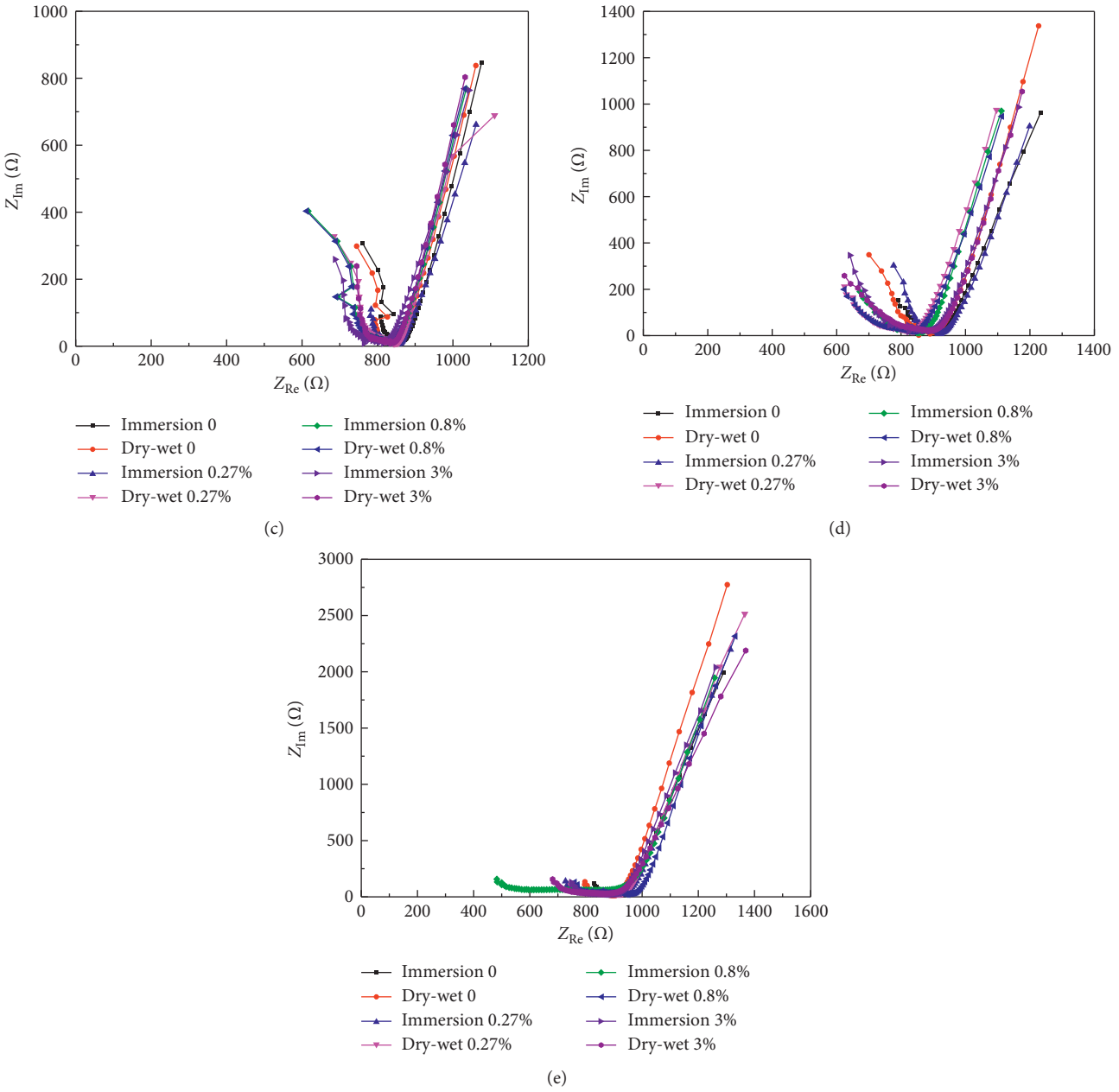

Figure 8: Nyquist diagram of reinforcement for flexural specimens at each age: (a) 60 days, (b) 120 days, (c) 180 days, (d) 240 days, and (e) 300 days.

by numerous scholars, indicating a typical feature of reinforcing steel in concrete in a passivated state [21–24]. Therefore, complete passivation film formed on the surface of the reinforcement concrete, and the reinforcement inside the flexural specimens at different corrosion ages and under different corrosion environments did not show any rusting. Comparing the Nyquist plot of the same age and different corrosive environments in the low-frequency band tolerance arc shows that the slope of the low-frequency band tolerance arc is basically the same, but the highest point of the low-frequency band tolerance arc is not significantly related to the concentration of boric acid corrosion solution, that is, the integrity of the passivation film on the surface of the steel is not affected by the concentration of the corrosion solution.

4.4. Effect on the Microstructure of Concrete. The sampled concrete powder was analyzed by X-ray diffraction (XRD) using a D8 ADVANCE X-ray diffractometer. A reinforced concrete specimen with a corrosion age of 300 days was selected and sampled on the surface and at 2 cm depth. Figure 9 shows the XRD analysis result. The XRD diffraction pattern shows that the corrosion product on the surface (0 cm) includes metaborate ($Ca(B0_2)_2$) and polyborate products (CaB_6O_{10}-$4H_2O$, CaB_4O_{10}). No significant

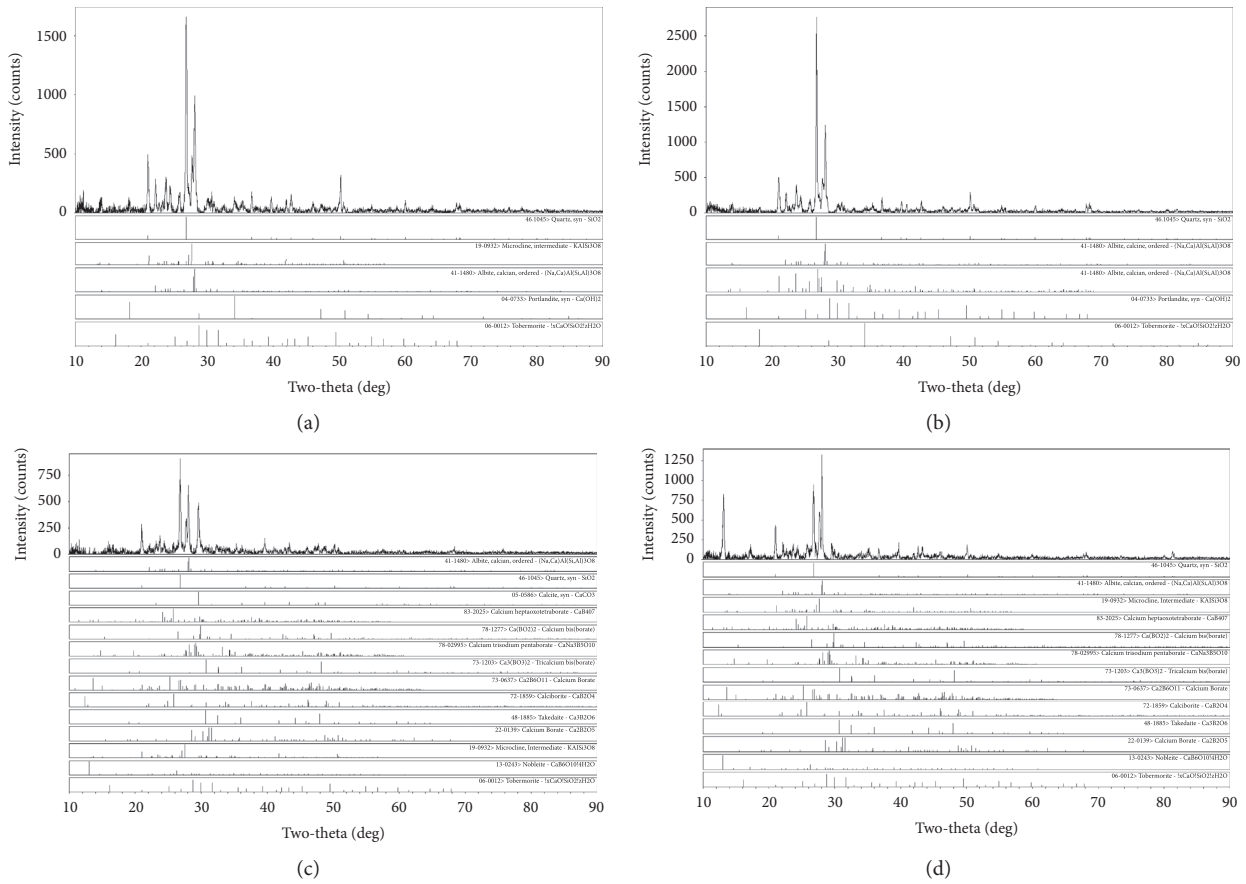

Figure 9: XRD analysis at 300 days of corrosion: (a) immersion 0.8% (2 cm), (b) immersion 3% (2 cm), (c) dry-wet 0.8% (0 cm), and (d) dry-wet 3% (0 cm).

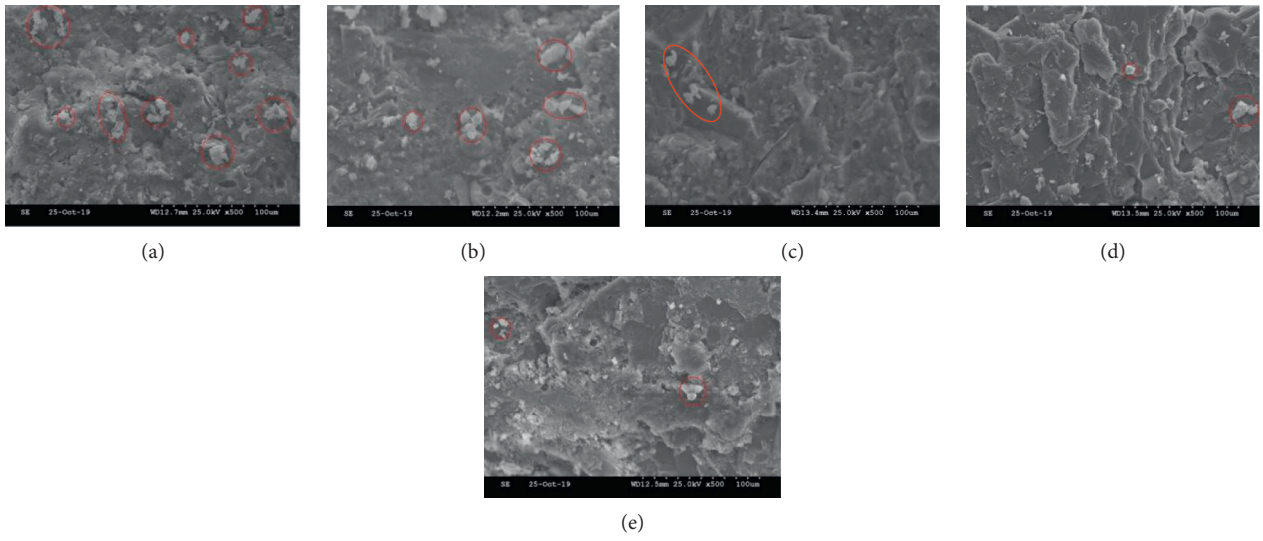

Figure 10: Electron microscopy scans of specimens at 300 days of corrosion: (a) immersion 0.8% (0 cm), (b) immersion 3% (0 cm), (c) immersion 0.27% (0 cm), (d) dry-wet 0.8% (2 cm), and (e) immersion 3% (2 cm).

corrosion products were detected in the diffraction pattern of the concrete internal specimens (2 cm). According to the relevant literature, boric acid produces metaborates with alkaline substances in an alkaline environment and polyborates with alkaline substances in an acidic environment. Boric acid mainly reacts with alkaline leaching solution and

has a weak corrosive effect on concrete specimens. The X-ray scan analysis results are consistent with the phenolphthalein solution color development results shown in Figure 6.

The concrete specimens were analyzed by scanning electron microscopy using an S-3500N series electron scanning microscope. Figure 10 shows the electron microscope scanning images of concrete specimens, indicating 0.8%, 3%, and 0.27% crystalline content of white corrosion products on the surface of the specimen under the immersion environment. The main reason is that the corrosion crystals attached to the surface of the specimen in the boric acid concentration of 3% environment inhibited the further corrosion of concrete. The concrete specimens did not show obvious corrosion crystallization products at 2 cm inside the specimen, allowing assuming that the corrosion of concrete by the boric acid mainly occurred on the concrete surface.

5. Conclusions

In conclusion, the corrosive effect of boric acid solution on reinforced concrete was systematically studied under two test environments, immersion and alternating wet-dry, to simulate the actual situation of nuclear power plant operation. The effects of boric acid corrosion on reinforced concrete were studied, leading to the following conclusions:

(1) The effect of the boric acid solution on the compressive strength, splitting tensile strength, elastic modulus, flexural strength, and bond strength of reinforced concrete specimens was found to be small. The corrosion effect is related to the concentration of the boric acid solution, but the effect is not significant. The corrosion degree of the specimens is mainly determined by the corrosion age.

(2) The effect of the boric acid solution on the yield strength, ultimate strength, and rust rate of steel bars and steel plates is weak, and the mechanical properties of the specimens after corrosion still met the strength requirements during the service.

(3) For concrete, the degradation of mechanical properties is slightly higher in alternating wet and dry environments than in the immersion environments; for example, the loss rate of compressive strength in these environments was 5.04% and 4.07%, respectively. However, steel specimens did not show this pattern.

(4) Corrosion occurs only at 2 cm inside the specimen under the action of boric acid.

(5) With increasing corrosion age, uneven corrosion products began to cover the surface of the specimen that inhibits further corrosion.

(6) The corrosion of reinforced concrete structures by boric acid has minimal impact on the safety of nuclear power plants, and thus, this study provides a reference for nuclear power plant operation and maintenance.

Data Availability

The data used to support the findings of this study are included within the article and also available from the corresponding author upon request.

Conflicts of Interest

The authors declare that they have no conflicts of interest.

Acknowledgments

This project was supported by the High-Level Talent Research Fund of Qingdao Agricultural University (663/1120050).

References

[1] Y. H. Zheng, *40 Years, Write a Brilliant Chapter in the Use of Nuclear Energy*, China Energy News, Zhejiang, China, 2018.

[2] L. Wang, T. S. He, Y. X. Zhou et al., "The influence of fiber type and length on the cracking resistance, durability and pore structure of face slab concrete," *Construction and Building Materials*, vol. 282, Article ID 122706, 2021.

[3] S. M. Abd El Haleem, S. Abd El Wanees, E. E. Abd El Aal, and A. Diab, "Environmental factors affecting the corrosion behavior of reinforcing steel II. Role of some anions in the initiation and inhibition of pitting corrosion of steel in $Ca(OH)_2$ solutions," *Corrosion Science*, vol. 52, no. 2, pp. 292–302, 2010.

[4] Z. S. Yao, Y. Fang, W. H. Kong, X. W. Huang, and X. S. Wang, "Experimental study on dynamic mechanical properties of coal gangue concrete," *Advances in Materials Science and Engineering*, vol. 2020, Article ID 8874191, 16 pages, 2020.

[5] C. Muñoz-Ruiperez, A. Rodríguez, C. Junco, F. Fiol, and V. Calderon, "Durability of lightweight concrete made concurrently with waste aggregates and expanded clay," *Structural Concrete*, vol. 19, no. 5, pp. 1309–1317, 2018.

[6] M. Kumar, A. K. Sinha, and J. Kujur, "Mechanical and durability studies on high-volume fly-ash concrete," *Structural Concrete*, vol. 22, no. 1, pp. 1–14, 2020.

[7] D. Chen, K. J. Howe, J. Dallman et al., "Experimental analysis of the aqueous chemical environment following a loss-of-coolant accident," *Nuclear Engineering and Design*, vol. 237, no. 20-21, pp. 2126–2136, 2007.

[8] W. Ramm and M. Biscoping, "Autogenous healing and reinforcement corrosion of water-penetrated separation cracks in reinforced concrete," *Nuclear Engineering and Design*, vol. 179, no. 2, pp. 191–200, 1998.

[9] A. Demirbaş and S. Karslioğlu, "The effect of boric acid sludges containing borogypsum on properties of cement," *Cement and Concrete Research*, vol. 25, no. 7, pp. 1381–1384, 1995.

[10] C. Z. Wu, R. F. Zhu, J. P. Lin et al., "Selection and application of AP1000 WIRST material," *Hot Working Techmolog*, vol. 44, no. 14, pp. 120–125, 2015.

[11] H. Huang, N. G. Jin, G. Y. Zheng et al., "Study on the influence of boric acid on the corrosion of concrete," *China Concrete and Cement Products*, vol. 3, pp. 14–16, 2006.

[12] H. Rong, L. Yang, J. W. Li et al., "Research on the corrosion effect on the durability of concrete structure of a nuclear power plant by boric acid," *Industrial Construction*, vol. 47, no. 9, pp. 35–38, 2017.

[13] L. Wang, M. M. Jin, Y. H. Wu et al., "Hydration, shrinkage, pore structure and fractal dimension of silica fume modified low heat Portland cement-based materials," *Construction and Building Materials*, vol. 272, Article ID 121952, 2021.

[14] L. Wang, R. Luo, and W. Zhang, "Effects of fineness and content of phosphorus slag on cement hydration, permeability, pore structure and fractal dimension of concrete," *Fractals*, vol. 29, no. 2, Article ID 2140004, 2021.

[15] L. J. Jiang, M. F. Chang, and Z. Q. Wen, "Experimental study on mechanical properties of corroded steel bars," *Low Temperature Architecture Technology*, vol. 33, no. 3, pp. 62–64, 2011.

[16] G. Xu, Z. W. Yang, R. Zhang et al., "Corrosion characteristics of rebar in two surface states under chloride environment," *Journal of Building Materials*, vol. 22, no. 2, pp. 254–259, 2019.

[17] Z. Y. Ai, J. Y. Jiang, W. Sun et al., "Passive behaviour of Cr_8Ni_2 alloy corrosion-resistant steel in simulating concrete pore solutions with different pH values," *Journal of Southeast University (Natural Science Edition)*, vol. 46, no. 1, pp. 152–159, 2016.

[18] S. Joiret, M. Keddam, X. R. Nóvoa, M. C. Pérez, C. Rangel, and H. Takenouti, "Use of EIS, ring-disk electrode, EQCM and Raman spectroscopy to study the film of oxides formed on iron in 1 M NaOH, ring-disk electrode, EQCM and Raman spectroscopy to study the film of oxides formed on iron in 1 M NaOH," *Cement and Concrete Composites*, vol. 24, no. 1, pp. 7–15, 2002.

[19] L. Yang, Z.-Q. Jin, and H. Zhang, "Steel corrosion electrochemical research under the condition of wet and dry cycle," *Concrete*, vol. 4, pp. 27–29, 2014.

[20] C. Xu, Z. Y. Li, and W. L. Jin, "Electrochemical impedance spectroscopy characteristics of corrosion behavior of rebar in concrete," *Corrosion Science and Protection Technology*, vol. 23, no. 5, pp. 393–398, 2011.

[21] G. Qiao and J. Ou, "Corrosion monitoring of reinforcing steel in cement mortar by EIS and ENA," *Electrochimica Acta*, vol. 52, no. 28, pp. 8008–8019, 2007.

[22] L. Wang, F. X. Guo, and Y. Q. Lin, "Comparison between the effects of phosphorous slag and fly ash on the C-S-H structure, long-term hydration heat and volume deformation of cement-based materials," *Construction and Building Materials*, vol. 250, Article ID 118807, 2020.

[23] M. Stern and A. Geary, "Electrochemical polarization I. A theoretical analysis of the shape of polarization curves," *Journal of the Electrochemical Society*, vol. 1, no. 104, pp. 56–63, 1957.

[24] S. G. Millard, D. Law, J. H. Bungey, and J. Cairns, "Environmental influences on linear polarisation corrosion rate measurement in reinforced concrete," *NDT & E International*, vol. 34, no. 6, pp. 409–417, 2001.